Asian Journal of Control, Vol. 18, No. 3, pp. 985–999, May 2016
Published online 16 July 2015 in Wiley Online Library (wileyonlinelibrary.com) DOI: 10.1002/asjc.1170

DIRECT POWER CONTROL OF DFIG BY USING NONLINEAR MODEL PREDICTIVE CONTROLLER

Nasrin Kalamian, Mohammad Verij Kazemi, and S. Asghar Gholomian

ABSTRACT

This paper proposes a nonlinear model predictive direct power control (PDPC) strategy for a double fed induction generator (DFIG)-based wind energy generation system. Active and reactive power variations of DFIG are calculated based on machine rules, and a nonlinear model of DFIG is given. A nonlinear model predictive controller (NMPC) is presented based on the useful cost function and constraint that it results in more proximity between simulations and reality. The power and current ripples are reduced and the optimal rotor voltage is generated based on an objective function and the constraints. The rotor voltage vector is calculated in the synchronous reference frame and transferred into the rotor reference frame. Simulation results of a 2 MW DFIG system show good performance of the proposed method during variation of active and reactive powers, machine parameters, and wind speed. Also, the transient responses of active and reactive powers are within a few milliseconds.

Key Words: Double fed induction generator, direct power control, nonlinear model predictive control

I. INTRODUCTION

The most important advantage of variable speed wind turbines versus a conventional constant speed system is improved dynamic behavior, resulting in reduction of the mechanical stress and fluctuation of the electrical power, and also increase in power capture [1]. One of the generation systems commercially available in the wind energy market is the doubly fed induction generator (DFIG), in which stator winding is directly connected to the grid and rotor winding is connected to the grid through a frequency converter (Fig. 1). One of the advantages of this system is the rating of the power converter, which is one third of the generator. Furthermore, it has four quadrants of active and reactive powers.

Direct torque control (DTC) of induction machines was developed in the mid 1980s [2,3]. DTC is an active research control scheme based on the decoupled control of flux and torque. DTC provides a very fast and precise torque response without a complex field-orientation block and inner current regulation loops. Based on the principles of DTC strategy, direct power control (DPC) was developed for DFIG. DPC directly controls the stator active and reactive power. One of the advantages of DPC is that it requires no extra current control loops, thereby simplifying the system design and enhancing the transient performance. Several researchers have focused on the progress of the DPC techniques that operate at a variable switching frequency [4,5]. Expensive and complicated AC harmonic filters and power converters are consequences of using the variable switching frequency. DPC at a constant switching frequency has been developed recently for the DFIG [6,7]. Nevertheless, the practical implementations of these methods are more complicated and expensive than conventional DPC. In [6], the authors focused on reduction of transient time and there is no discussion about THD of currents or the upper limit of robustness. Also, the rotor voltage of their method is not optimal. Their equations are not exact because they surrender some parameters, such as rotor resistance. Verijkazemi *et al*. [8] presented a new DPC on the basis of the DSVM technique. Then, in [9], this idea was improved by rearranging the sequence of the voltage space vectors and combining the fuzzy sets.

Model predictive controller as an optimal control method has been used for the DTC problem of three-phase induction motor drives [10]. The proposed method in [10] is a systematic design procedure based on maintaining variables within certain bounds while considering their feasibility. For calculating the control input, two methods are proposed: online computation and offline computation of the state-feedback control law. PDPC was proposed for DC/AC converters in [11]. The main idea of this paper is combining DPC with a predictive selection of voltage vector to achieve high transient dynamic and constant switching frequency. The authors consider predictive DPC based on two- and three-voltage vector sequences.

Antoniewicz *et al*. proposed PDPC for a three-phase boost rectifier [12]. First, six active and two zero voltage vectors are generated by the rectifier. Then, the predictive controller chooses the most effective vector by minimizing a cost function. Finally, the classical switching table and

Manuscript received September 15 2013; revised July 27 2014; accepted September 26 2014.

N. Kalamian is with Institute for Higher Education Pooyesh Qom, Electrical and Computer Department, Qom, Iran.

M. Verij Kazemi (corresponding author, e-mail: mohammad_v_kazemi@yahoo.com) and S. A. Gholomian are with Faculty of Electrical and Computer Engineering, Babol University of Technology, Babol, Iran.

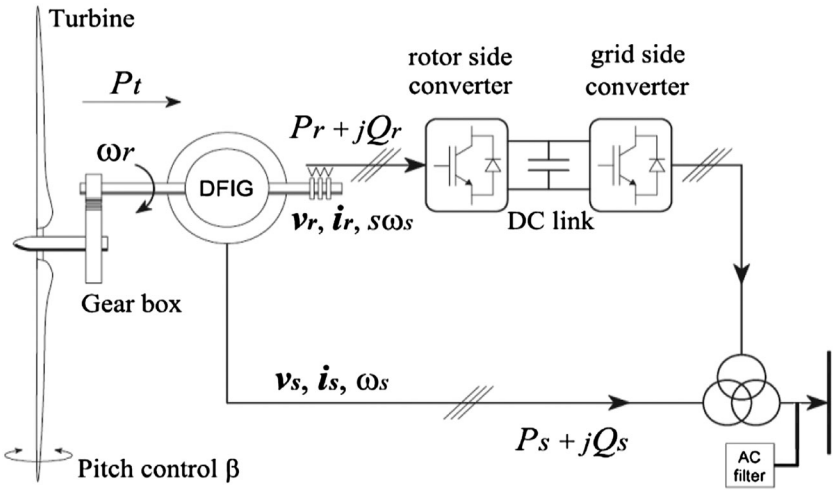

Fig. 1. Schematic of a DFIG-based wind generation system.

the proposed method are compared, and simulation results show lower THD in the proposed method.

Predictive direct torque control (PDTC) of the DFIG is presented in [13]. In this paper, the authors tried to reduce electromagnetic torque and flux ripples at a constant switching frequency. Using a switching table, voltage vectors are created, and with minimization of torque and flux ripple criteria, the best vector is chosen. The authors improved their method and achieved better results in [14].

In [15], a predictive control algorithm was presented for a three-phase active rectifier with line current harmonic spectrum control. Behavior of active and reactive powers in [6] is predicted and the suitable voltage vector is calculated by minimization of an objective function. Also, digital filters are added in order to form line current harmonic spectrum. The experimental results show better performance than classic DPC. Aurtenechea *et al*. used a predictive strategy to control DC/AC converters based on direct power control [16]. To achieve good transient and constant switching frequency, an optimal voltage vector is selected between three voltage vectors in a symmetrical way, which is called a symmetrical 3 + 3 vector sequence. The results show improvement in transient time and harmonic spectrum.

The PDPC has been employed to control MV-grid-connected two-level and three-level NPC converters [17]. The direct power control idea is admixture by prediction of a voltage vector sequence. The results show good transient dynamic and constant switching frequency on high power converters. Zhi *et al*. proposed PDPC for DFIG [18]. The main goal is that the errors of active and reactive powers become zero by selecting a suitable voltage vector by space vector modulation. One of the advantages of PDPC is an optimal control input, which is not mentioned in [18]. In their paper, the numbers of voltage vectors are low, which limits selection of a suitable voltage vector. Also, the formulations of DFIG and calculation of power errors are approximate, which leads to imprecise responses.

The method that was proposed in [19] is based on input-output feedback linearization. After linearization, they used a linear simple model predictive controller. This approach just focused on optimal rotor voltage and they did not consider any other constraints, such as THD, ripples, or robustness. Because of the linearization of system equations and some simplifying, the quality of transient time is decreased, so there is sizeable overshoot or undershoot and lower speed in transient time.

This paper proposes a nonlinear model-based PDPC and constant switching frequency for a DFIG-based wind turbine. The main advantage of the proposed method is that it increases performance while considering some constraints in the nonlinear model predictive controller (NMPC) structure. For these limits, basic factors are considered, such as THD and ripple reduction. So, NMPC chooses the optimal rotor voltage to achieve minimal tracking errors and to satisfy constraints, even during changing rotor speed, power references, and machine parameters.

The most important differences between our work and the work of others is presenting a new cost function and realizable constraints. To prove this claim, we compare our simulation results with three papers, that is, [9], [18], and [20]. In [18], there are no distinct constraints and the rotor voltage has more swinging and reaches maximum value more times. Also, THD in currents are bigger than our method and, with existing uncertainties in machine parameters, tracking errors and ripples become bigger. These problems come from the nonexistence of rich constraints and the cost function. Actually, in other papers, authors have focused on a special characteristic of DFIG and have proposed a control method to improve it. Nevertheless, using

NMPC can satisfy several goals in DFIG and improve them, such as characteristics of transient state (settling time, rise time, over or undershoot, and dead time), steady state tracking error, ripples in power and current, THD in current, slow swinging in rotor voltage, *etc*. during changing rotor speed or uncertainties in machine parameters. In this paper, the main goals, tracking error, and minimum rotor voltage are considered as the cost function and other lateral goals can be considered as constraints. So, with NMPC, one can improve the performance of DFIG, even under unknown or problematic conditions.

This paper will proceed as follows. In Section 2, the dynamic equations of DFIG are presented. First, the rotor voltage vector is calculated in synchronous reference frame and is transferred to the rotor reference frame. In this formulation, rotor and stator resistances are considered, whereas they have been disregarded in other papers for simplification. Second, these formulas are denoted as discrete time state space form for use in the NMPC part. The state space is a useful and popular form that can be used in most of the other control methods. The NMPC approach and its details are introduced in Section 3. The main advantage of NMPC is that every change in the reference trajectory is seen before its time, so the controller can react quickly, making transient time and overshoot minimal. The other benefits of NMPC are creation of the optimal control input and reduction of energy consumption. Also, other lateral goals can be considered as constraints (that have never been used before), such as reduction of ripple power and THD of stator and rotor currents. The hybrid NMPC-DPC provides more proximity between simulations and reality. In this section, the elements of NMPC, prediction model, objective function, and constraints are investigated in detail. Simulation results are presented in Section 4. These results show that active and reactive power can track their variable reference trajectories with small errors and good transient state, even under rotor speed variation. The robustness of the proposed method is analyzed by increasing all inductances. The results show that, even under existing uncertainties, tracking errors are small and acceptable.

II. Dfig Nonlinear Model

The stator voltage vector in the synchronous d–q reference frame is given as,

$$V_s = R_s I_s + \frac{d}{dt}\psi_s + j\omega_1\psi_s \tag{1}$$

where ω_1 is synchronous angular frequency and ψ_s, V_s, I_s, R_s are the flux, voltage, current, and resistance of the stator, respectively. Under a balanced AC voltage supply, the amplitude and rotation speed of the stator flux are constant. Therefore, in the synchronous d–q frame, the stator flux maintains a constant value. As shown in Fig. 2, if the d-axis of the synchronous frame is fixed with the stator flux vector, there is

$$\psi_s = \psi_{sd} \tag{2}$$

$$\frac{d}{dt}\Psi_s = 0 \tag{3}$$

In the synchronous reference frame, the stator and rotor flux are expressed as

$$\begin{aligned}\Psi_s &= L_s\ I_s + L_m\ I_r \\ \Psi_r &= L_r\ I_r + L_m\ I_s\end{aligned} \tag{4}$$

where ψ_r, I_r are the flux and current of the rotor and where L_r, L_s, L_m are the rotor and stator self-inductance and mutual inductance, respectively. Based on (4) the stator current is given as

$$I_s = \frac{L_r\psi_s - L_m\psi_r}{\sigma L_r L_s} \tag{5}$$

where $\sigma = \frac{L_r L_s - L_m{}^2}{L_r L_s}$

According to 2–5, the instantaneous stator active and reactive power outputs from the DFIG to the network side can be calculated as

$$\begin{aligned}P_s - jQ_s &= \frac{3}{2}\ [V_s]^*[I_s] \\ P_s - jQ_s &= \frac{3}{2}\ [R_s\ I_s + j\omega_1\psi_s]^*\left[\frac{L_r\psi_s - L_m\psi_r}{\sigma L_r L_s}\right] \\ P_s - jQ_s &= \frac{3}{2}\ \left[R_s\ \left(I_d + jI_q\right) + j\omega_1\psi_{sd}\right]^*\left[\frac{L_r\psi_{sd} - L_m\left(\psi_{rd} - j\psi_{rq}\right)}{\sigma L_r L_s}\right] \\ P_s - jQ_s &= \frac{3}{2}\ \left[R_s\ I_d + j\left(R_s\ I_q + \omega_1\psi_{sd}\right)\right]^*\left[\frac{L_r\psi_{sd} - L_m\psi_{rd}}{\sigma L_r L_s} + j\frac{L_m\psi_{rq}}{\sigma L_r L_s}\right] \\ P_s - jQ_s &= \frac{3}{2}\ \left[R_s\ I_d + j\left(R_s\ I_q + \omega_1\psi_{sd}\right)\right]^*\left[\frac{L_r\psi_{sd} - L_m\psi_{rd}}{\sigma L_r L_s} + j\frac{L_m\psi_{rq}}{\sigma L_r L_s}\right]\end{aligned} \tag{6}$$

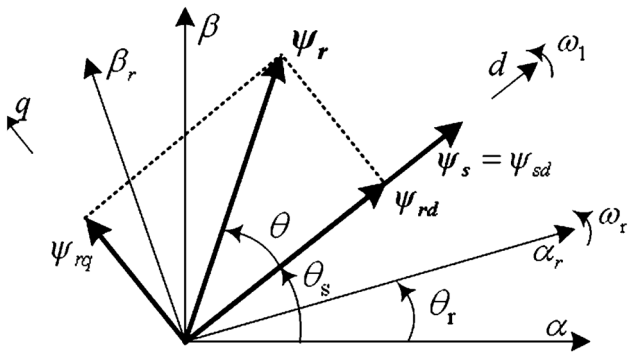

Fig. 2. Stator and rotor flux vectors in the synchronous d–q frames.

where R_r is the resistance of the rotor. Splitting (6) into real and imaginary parts yields

$$\begin{aligned} P_s &= \frac{3}{2}\left[\frac{R_s\ I_d\left(L_r\psi_{sd}-L_m\psi_{rd}\right)-L_m\psi_{rq}\left(R_s\ I_q+\omega_1\psi_{sd}\right)}{\sigma L_r L_s}\right] \\ Q_s &= -\frac{3}{2}\frac{R_s\ I_d L_m\psi_{rq}+\left(R_s\ I_q+\omega_1\psi_{sd}\right)\left(L_r\psi_{sd}-L_m\psi_{rd}\right)}{\sigma L_r L_s} \end{aligned} \tag{7}$$

If, in (7), all parameters are known except the rotor flux, according to other parameters, ψ_{rd}, ψ_{rq} can be obtained.

$$\begin{aligned} \psi_{rq} &= -a\left[R_s\ \left(P_s I_q+Q_s I_d\right)+\omega_1\psi_{sd}P_s\right] \\ \psi_{rd} &= a\left[R_s\ \left(-P_s I_d+Q_s I_q\right)+\omega_1\psi_{sd}Q_s\right]+\frac{L_r}{L_m}\psi_{sd} \end{aligned} \tag{8}$$

Where $a=\frac{\sigma L_r L_s}{L_m\left[R_s\ ^2 I_d{}^2+\left(R_s\ I_q+\omega_1\psi_{sd}\right)^2\right]}$

According to (3) the amplitude of stator flux is assumed constant during one sample time. Also the voltage drop in stator resistance is neglected. Therefore, according to (7), the active and reactive power changes over a constant period of T_s are given by

$$\begin{aligned} \Delta P_s &= -\frac{3}{2}\frac{R_s\ I_d L_m}{\sigma L_r L_s}\Delta\psi_{rd}-\frac{3}{2}\frac{L_m\left(R_s\ I_q+\omega_1\psi_{sd}\right)}{\sigma L_r L_s}\Delta\psi_{rq} \\ \Delta Q_s &= \frac{3}{2}\frac{L_m\left(R_s\ I_q+\omega_1\psi_{sd}\right)}{\sigma L_r L_s}\Delta\psi_{rd}-\frac{3}{2}\frac{R_s\ I_d L_m}{\sigma L_r L_s}\Delta\psi_{rq} \end{aligned} \tag{9}$$

Based on (9), within the period of T_s, the changes of rotor flux in the d- and q-axis are given by

$$\begin{aligned} \Delta\psi_{rq} &= -a\left[R_s\ \left(\Delta P_s I_q+\Delta Q_s I_d\right)+\omega_1\psi_{sd}\Delta P_s\right] \\ \Delta\psi_{rd} &= a\left[R_s\ \left(-\Delta P_s I_d+\Delta Q_s I_q\right)+\omega_1\psi_{sd}\Delta Q_s\right] \end{aligned} \tag{10}$$

The rotor voltage vectors are given in the synchronous reference frame as

$$\frac{d}{dt}\psi_r = V_r - R_r\ I_r - j\omega_s\psi_r \tag{11}$$

where $\omega_s=\omega_1-\omega_r$ is the slip frequency. Based on (11), the rotor voltage changes in synchronous d–q reference frame must follow

$$\begin{aligned} \frac{\Delta\psi_{rd}}{\Delta t} &= V_{rd}-R_r\ I_{rd}+\omega_s\psi_{rq} \\ \frac{\Delta\psi_{rq}}{\Delta t} &= V_{rq}-R_r\ I_{rq}-\omega_s\psi_{rd} \end{aligned} \tag{12}$$

By substitution of (8) and (10) into (12)

$$\begin{aligned} &\begin{bmatrix}\frac{\Delta P_s}{T_s}\\ \frac{\Delta Q_s}{T_s}\end{bmatrix} = C^{-1}A\begin{bmatrix}P_s\\ Q_s\end{bmatrix}+C^{-1}B+C^{-1}\begin{bmatrix}V_{qr}\\ V_{dr}\end{bmatrix} \\ &A=\begin{bmatrix}-a\omega_s R_s I_q-a\omega_1\omega_s\psi_{sd} & -\omega_s R_s I_d\\ a\omega_s R_s I_d & -a\omega_s R_s I_q-a\omega_1\omega_s\psi_{sd}\end{bmatrix}; \\ &B=\begin{bmatrix}-\frac{L_r}{L_m}\omega_s\psi_{sd}-R_r I_{rq}\\ -R_r I_{rd}\end{bmatrix}; \\ &C=\begin{bmatrix}-a\left(R_s I_q+\omega_1\psi_{sd}\right) & aR_s I_d\\ -aR_s I_d & a\left(R_s I_q+\omega_1\psi_{sd}\right)\end{bmatrix}; \end{aligned} \tag{13}$$

in this equation C is invertible because

$$|C|=-a^2(R_s I_q+\omega_1\psi_{sd})^2+a^2(R_s I_d)^2=a^2$$
$$((R_s I_d)^2-(R_s I_q+\omega_1\psi_{sd})^2).$$

If $a\neq 0$, then $|C|\neq 0$. The parameters $a=\frac{\sigma L_r L_s}{L_m\left[R_s{}^2 I_d{}^2+\left(R_s I_q+\omega_1\psi_{sd}\right)^2\right]}$ and $\sigma=\frac{L_r L_s-L_m^2}{L_r L_s}$ where $L_r\neq 0, L_s\neq 0$. If $L_r L_s\neq L_m^2$, then $\sigma\neq 0, a\neq 0$.

Rotor voltage with the use of (13) can be calculated so that the active and reactive powers return to the desired value. The required rotor output voltage in the synchronous reference frame is obtained, and it must be transformed into the rotor reference frame. This is achieved using the following

$$V_r^r = V_r e^{j(\theta_s-\theta_r)} \tag{14}$$

where θ_s, θ_r are stator and rotor flux angles in the stationary reference frame.

III. NONLINEAR MODEL PREDICTIVE CONTROL APPROACH

The NMPC method, based on minimizing a cost function under some constraints, seems to be very suitable for DFIG control. The NMPC is a general control scheme that is designed to solve a sequence of optimal control problems under some constraints [21]. NMPC consists of two parts: a nonlinear model and an optimizer, which requires an objective function with possible constraints. One difference between the predictive approach and other control strategies is that predictive control does not use the history of errors to produce a control input. Actually, this method considers the behavior of the system in the future instead of its past. This property leads to an optimal decision and also causes

the predictive control to permit an online method for calculation control input.

As shown in Fig. 3, following a reference trajectory by system output in the prediction horizon, future output is predicted using previous inputs and outputs. With this new information and reference path, disturbances, and control strategy, a group of adequate control inputs is calculated in the control horizon for suitable system performance. On the other hand, in the predictive control approach, the input signal is generated in several future steps as the system output converges to a desired trajectory in several future steps. The prediction horizon (N_p) is a time bound where the future output is forecast. The control horizon (N_c) is the number of steps where the sequence of control inputs is calculated.

In this method, in every sample, based on previous measurements until second k, using an open-loop system model, the controller predicts the output (N_p samples) and generates the control input (N_c samples ($N_c \le N_p$)) as the cost function becomes minimal (optimization). For consideration of feedback in a system, the first control input is given to the system in the next sampling. In the next sample, based on new measurement, the whole prediction and optimization process is repeated.

In a theoretical approach, the predictive control algorithm can be presented as an optimization problem [21]

$$u^* = \arg\min_u (J(k)) \tag{15}$$

$$\begin{aligned}
&\mathbf{X}(k|k) = \mathbf{X}_0 \\
&\mathbf{X}(k+j+1|k) = f_d(\mathbf{X}(k+j|k), \mathbf{u}(k+j|k)) \\
&\mathbf{Y}(k+j+1|k) = h_d(\mathbf{X}(k+j|k)) \\
&\mathbf{X}_{\min} \le \mathbf{X}(k+j|K) \le \mathbf{X}_{\max} \\
&\mathbf{u}_{\min} \le \mathbf{u}(k+j|K) \le \mathbf{u}_{\max} \\
&\mathbf{u}(k+j|k) = \mathbf{u}(k+N_C|k), j \ge N_C
\end{aligned} \tag{16}$$

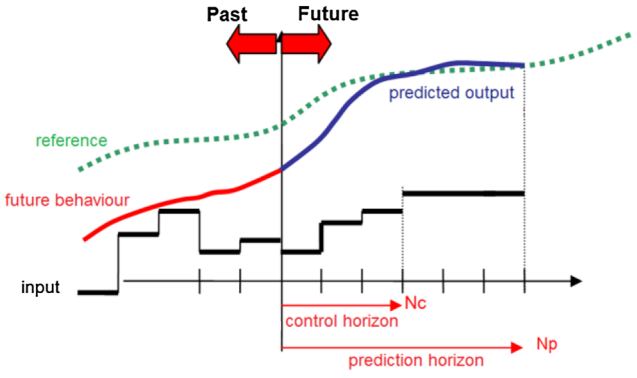

Fig. 3. General model predictive control.

where $j \in [0 \quad N_p - 1]$, $\mathbf{X}$ and $\mathbf{Y}$ are state and output vectors, respectively, and $\mathbf{u}$ is the control input. $a(m|n)$ is shown as variable a in second m that is predicted in second n. $\mathbf{X}_0$ is the initial state vector, and f_d and h_d are the system models that are needed for prediction. $[\mathbf{X}_{\min} \quad \mathbf{X}_{\max}]$ and $[\mathbf{u}_{\min} \quad \mathbf{u}_{\max}]$ are lower and upper limits of states and control input, respectively.

The optimization problems (15) and (16) are solved in every sample k and lead to a subsequent control input $\{\mathbf{u}^*(k+1|K), \ldots, \mathbf{u}^*(k+N_C|K)\}$. So, in the next sample $(k+1)$, the first element of the achieved subsequent control input $\mathbf{u}^*(k+1|K)$ is given to the system and, at the same time, the optimization problem will be solved again.

Predictive control needs a method of system identification for forecasting future behavior. The model used for prediction can be the dynamic equations of the system. The problem with this method is either uncertainty or unmodeled structures. If measurement of uncertainties becomes big, identification and prediction face the possibility of instability. So, if there is great uncertainty in the dynamic model of a system, online model identification, such as a fuzzy system or neural network, is necessary while under control.

NMPC can be used for the nonlinear model or cost function with an order bigger than two (quadratic) or nonlinear constraints on inputs, output, and states. This method is more precise than the linear method. With an increasing number of constraints, however, this may lead to no exact solution of the optimal problem.

Some features of predictive control are given below [21]:

- simple problem formulation
- easy tuning of controller parameters, even when changing the cost function
- optimality
- inherent delay compensation
- ability of consideration of constraints on inputs and outputs
- capability of popularization to multi-input multi-output
- profitable for non-minimum phase systems

In this paper, we propose an NMPC for DFIG. The most important differences between our work and others are presenting new modeling of DFIG, cost function, and realizable constraints. To prove this claim, we compare our simulation results with four papers, including [18]. In [18], there are no distinct constraints and the rotor voltage has more swinging and attains its maximum value in more iterations. Also, THD in currents is bigger than our method and, with existing uncertainties in machine parameters, tracking errors and ripples become bigger. These problems come from the nonexistence of rich constraints and cost function. These improvements are shown in Figs. 6 and 7 and in Tables II and III.

As mentioned, predictive control has two important tasks: 1) identification and prediction based on the system model and 2) calculation of optimum control input for providing control requests. These two tasks are described next.

3.1. Prediction Model

Prediction of future states can be achieved in different ways. If the dynamic equations of a system do not change much over time, using a discrete system model is a very good choice. In this paper, the dynamic model of a DFIG is employed. It is assumed that the state vector $\mathbf{X}(t) = [P_s(t) \quad Q_s(t)]^T$ is available in every moment, then the approximate equation can be written as

$$\mathbf{X}(t+\Delta t) = \begin{bmatrix} P_s(t+\Delta t) \\ Q_s(t+\Delta t) \end{bmatrix} \approx \begin{bmatrix} \dot{P}_s(t).\Delta t + P_s(t) \\ \dot{Q}_s(t).\Delta t + Q_s(t) \end{bmatrix} \quad (17)$$

where Δt is the sampling period. Whenever Δt becomes smaller, approximation will be more precise. $\dot{P}_s(t), \dot{Q}_s(t)$ are variations of active and reactive powers that are calculated by

$$\begin{bmatrix} \dot{P}_s(t) \\ \dot{Q}_s(t) \end{bmatrix} = C^{-1}A \begin{bmatrix} P_s(t) \\ Q_s(t) \end{bmatrix} + C^{-1}B + C^{-1} \begin{bmatrix} V_{qr}(t) \\ V_{dr}(t) \end{bmatrix} \quad (18)$$

where A, B, C were given in (13). With knowledge of $\mathbf{V}_r(t)$ that is earned from the controller, in every moment the future state vector (next moment) can be calculated. To predict the next few steps, recessive repetition of the aforementioned equations can be used.

3.2. Objective Function

Different predictive control algorithms use different cost functions to calculate the control input. The main goal is the flow of future output from the reference trajectory in a special horizon. Also, the control input should be minimized. General expansion of this objective function is as follows

$$J(N_1, N_2, N_u) = \sum_{i=N_1}^{N_2} \delta(i)[\hat{y}(t+i|t) - w(t+i)]^2 + \sum_{i=1}^{N_u} \lambda(i)[\Delta u(t+i-1)]^2 \quad (19)$$

In this cost function, the following can be mentioned:

1. **Parameters:** N_1 and N_2 are minimum and maximum, respectively, of the cost horizon, and N_u is the control horizon that does not have to be equal to the maximum horizon.
2. **Reference trajectory:** one of the advantages of predictive control is that future variation of the desired signal can be detected and the algorithm can reflect it, so delay effects can be reduced in the system response.
3. **Constraints:** in reality, every signal has limitations. These limitations in dimension and variation rate of control input and output constraints are considered as below

$$\begin{aligned} &u_{\min} \le u(t) \le u_{\max} && \forall t \\ &du_{\min} \le u(t) - u(t-1) \le du_{\max} && \forall t \\ &y_{\min} \le y(t) \le y_{\max} && \forall t \end{aligned} \quad (20)$$

There are two main goals that are considered in the cost function in this paper: 1) tracking of active and reactive power references with acceptable error and 2) minimizing energy consumption.The cost function can be written as

$$\begin{aligned} J = {} & w_1 \sum_{i=0}^{N_c-1} \mathbf{V_r}(t+i\Delta t)^T \mathbf{V_r}(t+i\Delta t) \\ & + w_2 \sum_{i=1}^{N_p} \left[P_s(t+j\Delta t) - P_s^{ref}(t+j\Delta t)\right]^2 \\ & + w_3 \sum_{i=1}^{N_p} \left[Q_s(t+j\Delta t) - Q_s^{ref}(t+j\Delta t)\right]^2 \end{aligned} \quad (21)$$

where $\mathbf{V_r}(t+\mathrm{i}\Delta\mathrm{t})$ is the rotor voltage vector at the $t+\mathrm{i}\Delta\mathrm{t}$ second (i th sample). $P_s(t+\mathrm{j}\Delta\mathrm{t})$ and $Q_s(t+\mathrm{j}\Delta\mathrm{t})$ are active and reactive powers at the $t+\mathrm{j}\Delta\mathrm{t}$ second (j th sample), respectively. $P_s^{ref}(t+\mathrm{j}\Delta\mathrm{t})$ and $Q_s^{ref}(t+\mathrm{j}\Delta\mathrm{t})$ are references of active and reactive powers at the $t+\mathrm{j}\Delta\mathrm{t}$ second, respectively. The parameters N_p and N_c are the prediction and control horizons. Δt is the sampling time, and w_1, w_2, and w_3 are the weights for the required rotor voltage and tracking the desired active and reactive powers, respectively.

In Fig. 4, the general schematic of the presented method is shown. $\begin{bmatrix} P_s(k) \\ Q_s(k) \end{bmatrix}$ and $\begin{bmatrix} P_s(k+1) \\ Q_s(k+1) \end{bmatrix}$ are active and reactive powers in samples k and $k+1$. $V_r(k+1)$ is the rotor voltage in sample $k+1$.

In this paper, the optimization problem is solved by the *fmincon* MATLAB function, which is a numerical nonlinear multi-objective optimization solver. This function is based on sequential quadratic programing (SQP) and can be used with nonlinear equality or inequality constraints. In the SQP method, the problem is divided as some quadratic programing and solved at each sample time.

3.3. Constraints

As mentioned, NMPC can minimize a cost function while satisfying some constraints. These limits can improve

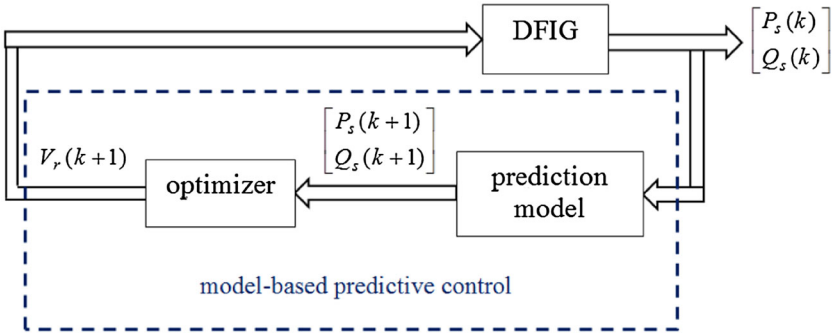

Fig. 4. General schematic of presented method.

system performance. In this paper, the error of active and reactive powers and the optimal voltage vector are considered in the objective function. Also, ripples of active and reactive powers and THD reduction and voltage limitation are used in the constraints part as below.

1. The rotor voltage should be limited

$$|V_r| \le V_{r\max} \tag{22}$$

2. Reduction of active power ripples

$$\begin{aligned} &if\,|e_{Ps}| < \delta then \left|\frac{d(e_{P_s})}{dt}\right| \le \varepsilon \\ &if\,|e_{Ps}| > \delta then \left|\frac{d(e_{P_s})}{dt}\right| > \varepsilon' \end{aligned} \tag{23}$$

3. Reduction of reactive power ripples

$$\begin{aligned} &if\,|e_{Qs}| < \delta then \left|\frac{d(e_{Q_s})}{dt}\right| \le \varepsilon \\ &if\,|e_{Qs}| > \delta then \left|\frac{d(e_{Q_s})}{dt}\right| > \varepsilon' \end{aligned} \tag{24}$$

4. THD of stator current can be reduced

$$I_{sn} = \sum_{k=0}^{N-1} i_{sk} \times \exp\left(\frac{2\,\pi jkn}{N}\right) \tag{25}$$

$$THD_{Is} = \frac{\sqrt{I_{s2}{}^2 + I_{s3}{}^2 + \ldots I_{sn}{}^2}}{I_{s1}} \times 100\% \tag{26}$$

$$|THD_{Is}| \le \alpha \tag{27}$$

IV. SIMULATION RESULTS

The basic configuration of the proposed control strategy for a DFIG-based generation system is shown in Fig. 5. MATLAB/Simulink has been designed for simulation with sampling frequency 4 kHz. The DFIG is rated at 2 MW, and its parameters are given in Table I. The nominal converter dc link voltage ($V_{r\max}$) was set at 1200 V. Based on the proposed DPC strategy, the rotor side converter controls the DFIG stator's active and reactive powers.

The rotor side converter switching frequency is 1300Hz. The grid side converter has to maintain a constant dc link voltage, and it is controlled by a method similar to the dc voltage controller in a VSC transmission system [22] with a switching frequency of 4 kHz.

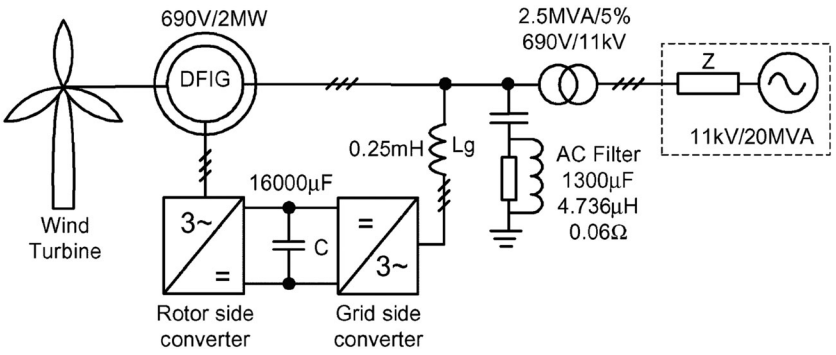

Fig. 5. Schematic of the simulated system.

Table I. Comparison of the distributions of the active and reactive power errors For $0.1 < t < 0.4$,Pref = -1.5 MW , Qref = -0.8MVar

	$\omega_r = 0.7$									
	ΔP					ΔQ				
Proposed method	[6]	[18]	[20]	[23]	In this paper	[6]	[18]	[20]	[23]	In this paper
Without uncertainties	.0094	.0054	.0092	.0090	.0033	.0092	.0042	.0091	.0098	.0035
With 50% increasing in all inductances	.0112	.0059	.0102	.0099	.0037	.0113	.0047	.0094	.0101	.0040
	$\omega_r = 1.3$									
Proposed method										
Without uncertainties	.0098	.0051	.0093	.0088	.0035	.0099	.0050	.0094	.0097	.0034
With 50% increasing in all inductances	.0111	.0055	.0099	.0099	.0036	.0116	.0057	.0103	.0101	.00038

At first, the grid side converter is enabled, such that the common dc link voltage is regulated. The DFIG stator then is energized with the rotor, which rotates at a regulated speed, and the rotor side converter is disabled. In the proposed method, the NMPC parameters are considered as below

$$N_p = 4; N_c = 3; w_1 = 1; w_2 = 0.5; w_3 = 0.1; \Delta t = 0.001; \varepsilon^{'} = 2{*}\varepsilon; \delta = 1\%; \alpha = 3\%$$

The simulation results of the nonlinear model predictive controller for a DFIG-based wind turbine are shown in Figs. 6 to 9. The reference trajectory of active and reactive powers is considered as a varying step. Initial active power is –0.6 MW, at 0.1 s changes to –2 MW, and at 0.2 s changes to –1 MW. Initial reactive power is –1MVar, at 0.15 s changes to –0-.2MVar, and finally changes to 0.6MVar at 0.3 s.

The most important contribution of our approach is in the definition of a new cost function and realizable constraints that lead to smaller and optimal rotor voltage, a few millisecond transient response of active and reactive powers, reduction of power and current ripples, smaller THD in current, and increasing robustness with existing uncertainty in all machine parameters. Also, with our cost function, it is possible to choose different premiership of active or reactive power. To compare the proposed method with other methods, [18], [20], and [9] are considered. In Figs. 6 and 7, four columns (A, B, C, and D) are shown, which show simulation results with the method proposed in this paper and the methods proposed in [18], [20], and [9], respectively. For better comparison of different methods, THD values for different methods are demonstrated in Table III. In this paper, the THD is calculated by Power GUI block in matlab/simulink.

The responses are divided into two, transient and steady states. In the transient state, under or overshoot amplitude, rise time, settling time, and dead time are important response characteristics. In the steady state, when response is settled, the steady state error is a noteworthy characteristic. As shown in Fig. 6.A.a, even with high variations of reference powers and rotor speed, the proposed method in this paper has a good transient state in active and reactive powers.

The overshoot is negligible. The settling time is less than a few milliseconds, and there is no tangible dead time. Although there are ripples with small amplitude in the steady state response, the mean of errors in active and reactive powers is zero, which means the power can track the references with no constant errors. The maximum of ripple in power is less than 2%, which is negligible in comparison with other methods. Fig. 6.A.b shows the initial rotor speed is 0.7p.u. then, in 0.1 s, it becomes bigger until 0.3 s, where it fixes at 1.3p.u. The error of active and reactive powers is shown in Figs. 6.A.c and 6.A.d, where one can see that, even in change times, the controller reacts quickly and follows the desired path with almost no overshoot, which is one of the advantages of the NMPC method because it can predict variations before they happen. The optimal rotor voltage (p.u.) is shown in Fig. 6.A.e in the d and q frames. As one can see, most of the time, the voltage is below its maximum, which makes minimum energy consumption. In every control method, it is very important to have minimum swinging of the control input. Fast swinging of the control input can damage actuators and sometimes it is not possible mechanically or physically. As shown, the proposed method generates rotor voltage with minimal swinging in comparison with other methods. The stator and rotor currents shown in Figs. 6.A.f and 6.A.g present small THD in rotor and stator currents. The THD is not visible in responses, so there is a calculation of THD in Table III that is considered later.

In Fig. 6.B, the method proposed in [18] is considered. The authors in [18] used PDPC for reduction tracking errors, but there are no distinct constraints. As shown, in the transient state, the settling time is about 8 milliseconds, but, in the method proposed in this paper, the settling time was less than a few milliseconds. Also, there are ripples with bigger amplitude in the steady state responses. The amplitude of ripple in powers is about 5.5%, which is triple that of the proposed method. In Fig. 6.B.e, the rotor voltage

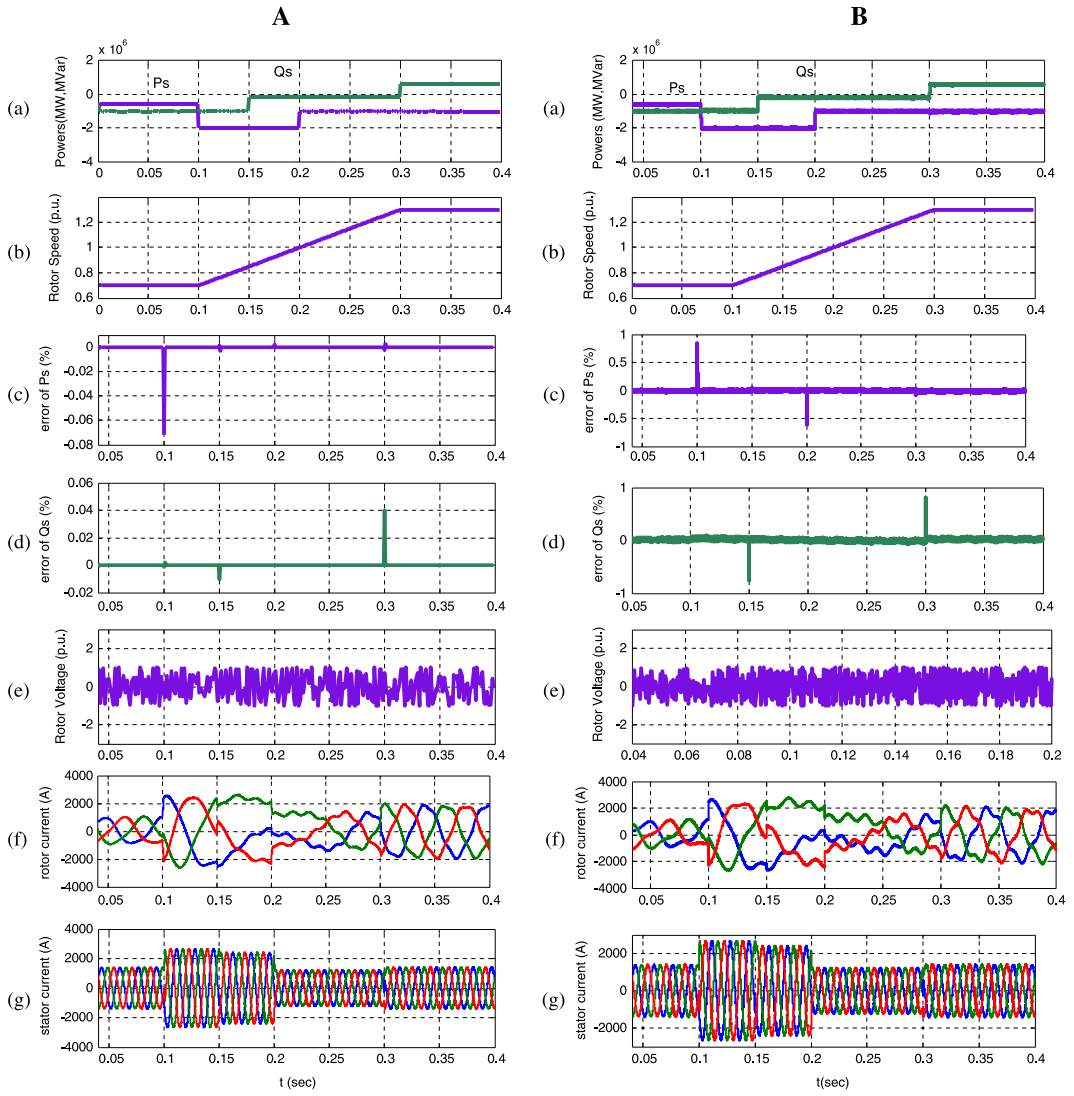

Fig. 6. Simulation results with proposed method in A) this paper, B) [18], C) [20], D) [9]: a) active and reactive powers (MW, MVar), b) rotor speed (p.u.), c) error of active power (%), d) error of reactive power (%), e) rotor voltage (p.u.), f) rotor current (kA), g) stator current (kA).

is shown. The rotor voltage is at a maximum value for more time. Furthermore, more swinging happens in the rotor voltage, which shows the rotor voltage in this method is not optimal. There is a possibility that sometimes this voltage cannot be available with this fast swinging. Figs. 6.B.f and g show stator and rotor currents. As has been noted, the THD is hard to see in responses, so there is a calculation of THD in Table III that shows this method has bigger THD in comparison with the proposed method.

In [20], a variable structure control method is implemented. The big problem with this method is chattering, which increases ripples and THD in power and current. Fig. 6.C shows that the chattering around reference value is considerable, which leads to bigger tracking errors and ripples. The chattering problem exists in all power, rotor voltage, and current levels and makes bigger THD. Nevertheless, this method has good speed for tracking references and the settling time is around 4 milliseconds, which is triple that of the method proposed in this paper. Because of the chattering problem, the rotor voltage is at maximum value most of the time and has faster swinging. Fuzzy-DPC is used in [9], and simulation results are shown in Column D. The tracking errors and ripples are acceptable but are not as small as the proposed method in this paper. The settling time is around 9 milliseconds, and the amplitude of ripple in powers is about 7%, which is much bigger than the method proposed in this paper. The rotor voltage acts in a similar way to the method proposed in this paper, and the speed of swinging and amplitude are better than in Columns B and D.

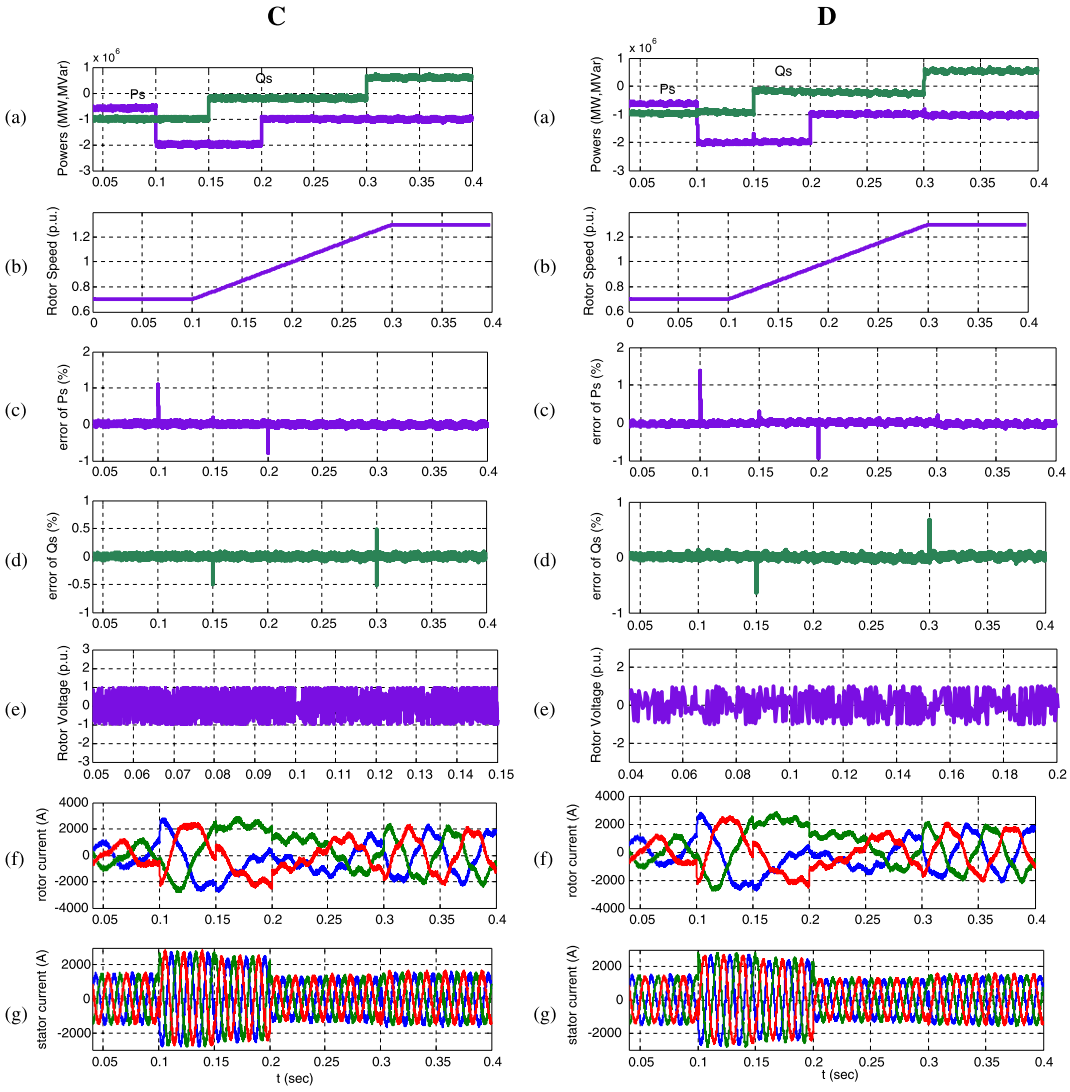

Fig. 6. (Continued)

As mentioned, the dynamic model of DFIG is considered a prediction model. This model may have some uncertainties that make it an imprecise model for prediction. So, in this paper, for investigation of uncertainty in parameters, all inductances increase 50% of their nominal.

Fig. 7.A.a shows the active and reactive powers with these uncertainties. Even with high variations of reference powers and rotor speed and uncertainties in parameters, the method proposed in this paper has good transient state in active and reactive powers. The overshoot is bigger than the no uncertainty state (3.5%) but it is still small. The settling time is less than 3.5 milliseconds, and there is no tangible dead time. Although there are ripples with small amplitude in the steady state response with existing uncertainties, the mean of errors in active and reactive powers is zero, which means the power can track the references with no constant errors. The tracking errors are shown in Figs. 7.A.c and 7.A.d. The controller has small tracking errors in change times, but responses are acceptable. The maximum of ripple in powers is around 2.5%, which, in comparison with other methods, is very good and a negligible percentage. The errors of active and reactive powers are shown in Figs. 7.A.c and 7.A.d, where one can see that, with these uncertainties, in change times, the controller has errors bigger than the no uncertainties state but the errors are still small in comparison with the other methods. The amplitude optimal rotor voltage is shown in Fig. 7.A.e in the d and q frames, and the proposed method generates rotor voltage with minimal swinging in comparison with other methods. The stator and rotor current are shown in Figs. 7.A.f and 7.A.g.

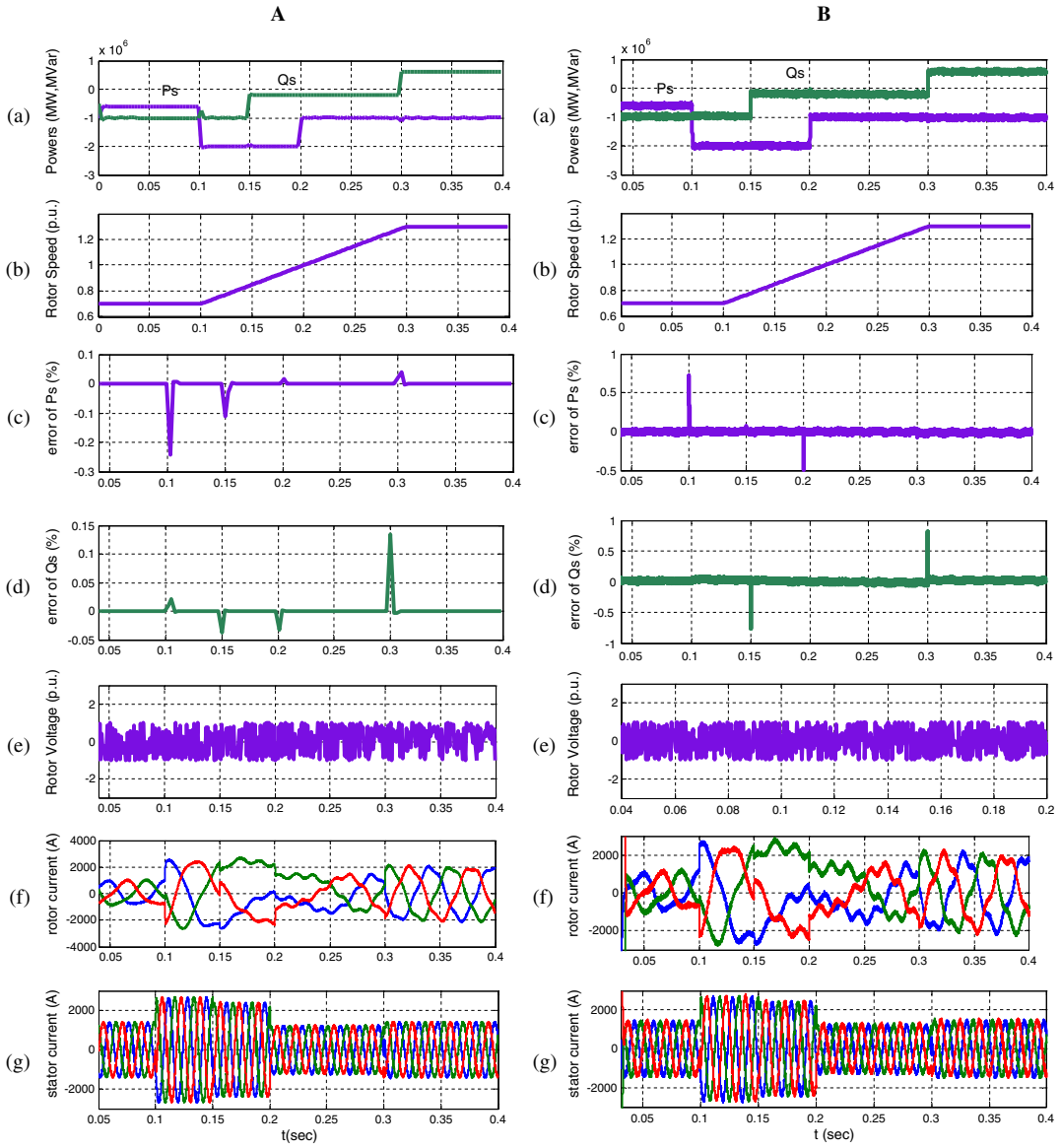

Fig. 7. Simulation results with 50% increasing all inductances: A) in this paper, B) in [18], C) in [20], D in: a) active and reactive powers (MW, MVar), b) rotor speed (p.u.), c) error of active power (%), d) error of reactive power (%), e) rotor voltage (p.u.), f) rotor current (kA), g) stator current (kA).

In Figs. 7.B, C, and D, the simulation results of [18], [20], and [9] are shown with the same uncertainties. In Fig. 7.B, there are ripples with bigger amplitude in the steady state responses. The amplitude of ripple in powers is about 6.5%, which is bigger than the method proposed in this paper. In Fig. 7.B.e, the rotor voltage is shown. The rotor voltage is at its maximum value for more time. Furthermore, more swinging occurs in the rotor voltage, which shows the rotor voltage in this method is not optimal. Figs. 7.B.f and g show stator and rotor currents.

Fig. 7.C shows that, in the variable structure method, chattering around the reference value is considerable, and this leads to bigger tracking errors, ripples, and THD. The settling time is around 4.5 milliseconds. Because of the chattering problem, the rotor voltage is at its maximum value most of the time and has faster swinging. Fig. 7.D shows that, in the fuzzy-DPC method, the tracking errors and ripples are acceptable but are not as small as in the method proposed in this paper. The settling time is around 12 milliseconds, and the amplitude of ripple in powers is about 8%, which is much bigger than the method proposed in this paper. The rotor voltage acts in an almost similar manner to the method proposed in this paper, and the speed of swinging and amplitude are better than in Columns B and

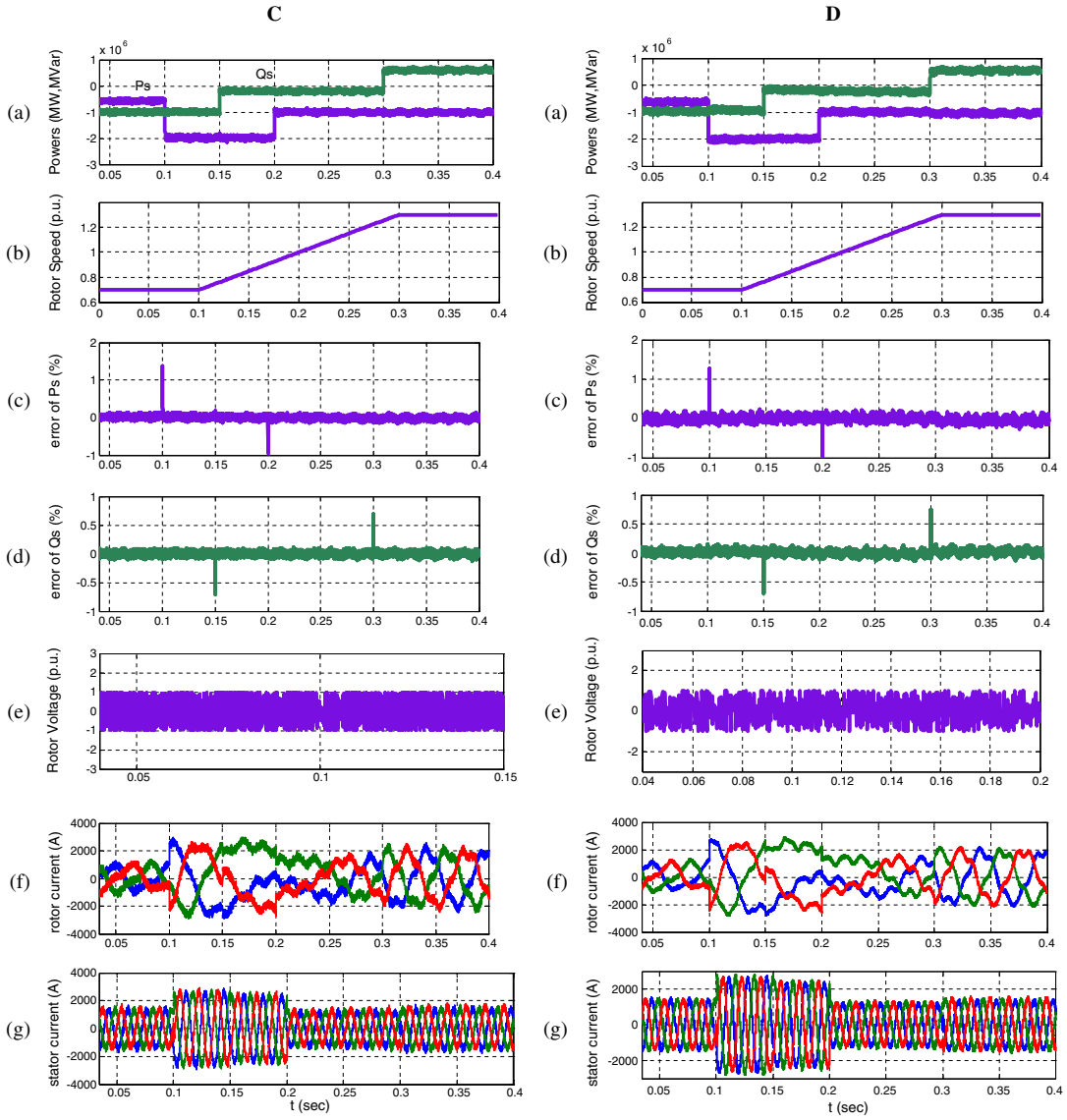

Fig. 7. (Continued)

D. For numerical comparison of ripples and errors, two parameters that were introduced in [9] are very useful. These parameters are $\Delta P = \int |P - P_{ref}| dt$ and $\Delta Q = \int |Q - Q_{ref}| dt$ in precise confined time for scrutiny of active and reactive power ripples. Table II shows these parameters in the proposed method for two modes: with and without 50% uncertainties in two different rotor speeds $\omega_r = 0.7$ and $\omega_r = 1.3$. To compare this paper with others, [6], [18], [20], and [23] are selected, and their results are also shown in Table II. One can see that the proposed method creates small and acceptable errors and ripples in active and reactive powers and currents. Simulation results on different conditions show that values of $\Delta P, \Delta Q$ with the method proposed in this paper are 31–67% lower than the methods proposed in other papers. Also, according to Table III, the THD of the stator currents in the proposed method is 18–47% lower than the methods proposed in [6], [18], [20], and [23].

In the proposed method, for best performance and to reduce calculation time, N_p and N_c are chosen small by trial and error ($N_p = 4, N_c = 3$). In Figs. 8 and 9, the effect of N_p

Table II. Comparison of the THD For $0.1 < t < 0.4$,$P_{ref} = -2$ MW , $Q_{ref} = -0.6$MVar, $\omega_r = 1.2$

Proposed method	[6]	[18]	[20]	[23]	In this paper
THD	5.07%	3.28%	4.18%	4.11%	2.68%

Table III. Parameters of the simulated DFIG

Rated power	2 MW
Stator voltage	690 V
Stator/rotor turns ratio	0.3
R_s	0.0108pu.
R_r	0.0121pu. (referred to the stator)
L_m	3.368pu.
$L_{\sigma s}$	0.11pu.
$L_{\sigma r}$	0.15pu. (referred to the stator)
Lumped inertia constant	0.2 s
Number of pole pairs	2

and N_c is investigated in the same situations and parameters. Fig. 8.A shows that, with an increasing prediction and control horizon ($N_p=6, N_c=5$), power tracking and errors do not have sensible changes, but one also can see in Fig. 9 that optimization time becomes bigger (in same parameters). As shown in Fig. 8.B, if N_p and N_c are chosen to be smaller, tracking errors and transient time become bigger. The coefficients of cost function are considered these numbers because of a preference for active power than reactive power and energy consumption.

V. CONCLUSION

This paper proposed a new nonlinear model-based PDPC strategy for a DFIG-based wind energy generation system. A new formulation of DFIG was used that considered all machine parameters, including resistances. This formulation makes a precise model of DFIG, which leads to production of an accurate control input. The rotor voltage vector is calculated in the synchronous reference frame and transferred to the rotor reference frame. An NMPC is presented based on the reduction of active and reactive power errors and energy consumption while satisfying some

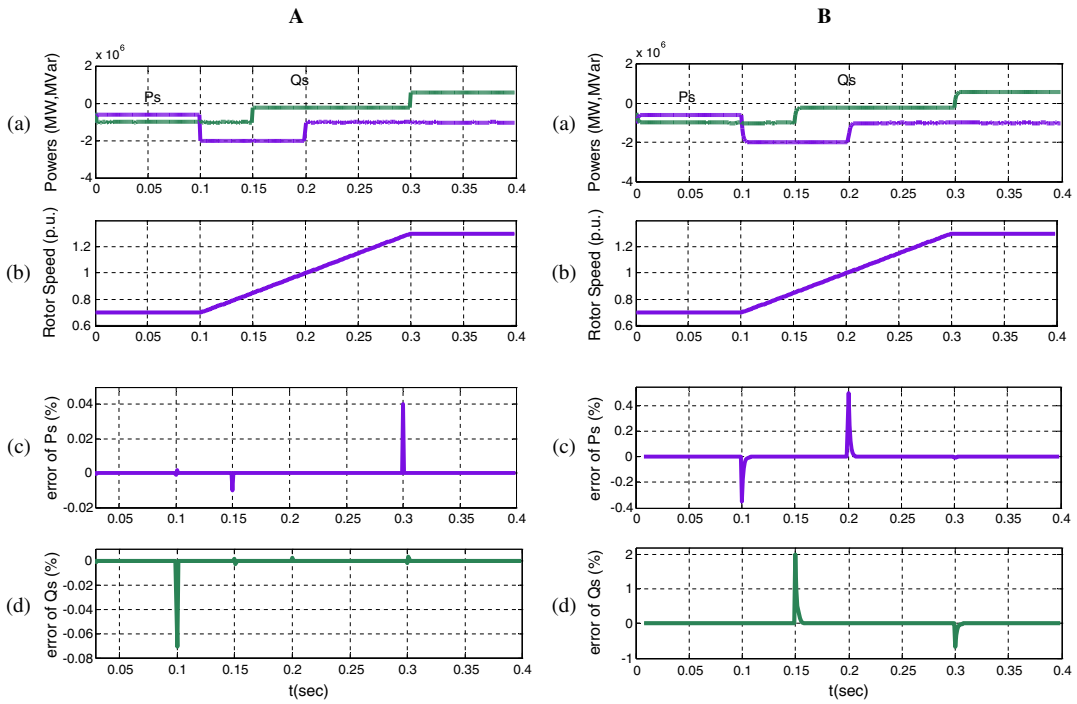

Fig. 8. A) $N_p=6, N_c=5$, B) $N_p=2, N_c=1$: a) active and reactive power, b) rotor speed, c) error of active power, d) error of reactive power.

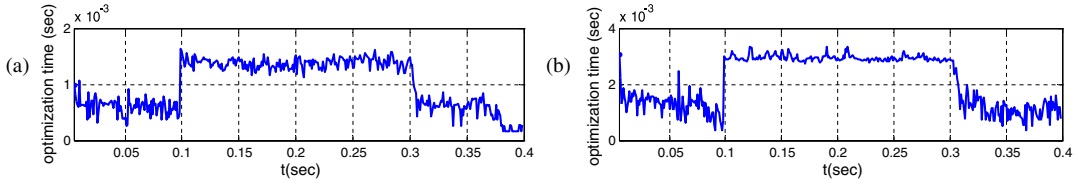

Fig. 9. Optimization time: a) $N_p=4, N_c=3$;b) $N_p=6, N_c=5$.

constraints. These constraints include ripples and THD reduction. Moreover, achieving these basic goals, the optimal nature of NMPC helps to calculate a suitable and optimal rotor voltage vector. Simulation results of a 2 MW DFIG system show good performance of the proposed method during variation of references of active and reactive powers and wind speed. The power and current ripples are reduced and the transient responses of active and reactive powers are within a few milliseconds and THD of stator current is suitable. The impact of machine parameter variations on system response was analyzed, and, from the results, it was found that this method can handle 50% increasing uncertainties in all inductances.

REFERENCES

1. Heier, S., *Grid Integration of Wind Energy Conversion Systems*, John Wiley & Sons, (1998).
2. Takahashi, I. and T. Noguchi, "A new quick-response and high-efficiency control strategy of an induction motor," *IEEE Trans. Ind.*, Vol. 41, No. 2, pp. 820–827 (1986).
3. Depenbrock, M., "Direct self-control (DSC) of inverter-fed induction machine," *IEEE Trans. Power Electron.*, Vol. 63, No. 3, pp. 420–429 (1988).
4. Datta, R. and V. T. Ranganathan, "Direct power control of grid-connected wound rotor induction machine without rotor position sensors," *IEEE Trans. Power. Electron.*, Vol. 16, No. 5, pp. 390–399 (2001).
5. Xu, L. and P. Cartwright, "Direct active and reactive power control of DFIG for wind energy generation," *IEEE Trans. Energy Convers.*, Vol. 21, No. 3, pp. 750–758 (2006).
6. Zhi, D. and L. Xu, "Direct power control of DFIG with constant switching frequency and improved transient performance," *IEEE Trans. Energy Convers.*, Vol. 22, No. 4, pp. 110–118 (2007).
7. Abad, G., Rodr´ıguez, M. A., and Poza, J., "Two-level VSC-based predictive direct power control of the doubly fed induction machine with reduced power ripple at low constant switching frequency," *IEEE Trans. Energy Convers.*, Vol. 23, No. 3, pp. 570–580 (2008).
8. Verij Kazemi, M., S. Yazdankhah, and H. M. Kojabadi, "Direct power control of DFIG based on discrete space vector modulation," *Renew. Energy*, Vol. 35, No. 2, pp. 1033–1042 (2010).
9. Verij Kazemi, M., M. Moradi, and R. Verij Kazemi, "Minimization of powers ripple of direct power controlled DFIG by fuzzy controller and improved discrete space vector modulation," *Int. J. Electr. Power syst. Res.*, Vol. 89, No. 5, pp. 23–30 (2012).
10. Geyer, T. and G. Papafotiou, "Direct torque control for induction motor drives: a model predictive control approach based on feasibility," *Hybrid Systems: Computation and Control*, Vol. 3414, No. 1, pp. 274–290 (2005).
11. Aurtenechea, S., M. A. Rodriquez, E. Oyarbide, and J. R. Torrealday, "Predictive direct power control – a new control strategy for DC/AC converters," *IEEE Ind. Electron. Conf.*, pp. 1661–1666 (2006).
12. Antoniewicz, P. and M. P. Kazmierkowski, "Predictive direct power control of three-phase boost rectifier," *Bull. Pol. Acad. Sci.-Tech. Sci.*, Vol. 54, No. 3, pp. 287–292 (2006).
13. Abad, G., M. A. Rodriguez, and J. Poza, "Predictive direct torque control of the doubly fed induction machine with reduced torque and flux ripples at low constant switching frequency," *IEEE Ind. Electron. Conf.*, pp. 1000–1005 (2006).
14. Sarasola, I., J. Poza, M. A. Rodriquez, and G. Abad, "Predictive direct torque control for brushless doubly fed machine with reduced torque ripple at constant switching frequency," *IEEE Ind. Electron. Conf.*, pp. 1074–1179 (2007).
15. Antoniewicz, P., M. P. Kazmierkowski, P. Cortes, J. Rodriguez, and A. Sikorski, "Predictive direct power control algorithm for three phase AC/DC converter," *EUROCON, The International Conf. on "Computer as a Tool"*, pp. 1530–1534 (2007).
16. Larrinaga, S. A., M. A. Rodriguez, E. Oyarbide, and J. R. Torrealday, "Predictive control strategy for DC/AC converter based on direct power control," *IEEE Trans. Ind. Electron.*, Vol. 54, No. 3, pp. 1261–1271 (2007).
17. Aurtenechea, S., M. A. Rodriguez, E. Oyarbide, and J. R. Torrealday, "Predictive direct power control of MV-grid-connected two-level and three-level NPC converters: experimental results," *Power Electron. and Appl. IEEE European Conf.*, pp. 1–10 (2007).
18. Zhi, D., L. Xu, and B. W. William, "Model predictive direct power control of doubly fed induction generators," *IEEE Trans. Power Electron.*, Vol. 25, No. 2, pp. 341–351 (2010).
19. Liu, X. and X. Kong, "Nonlinear model predictive control for DFIG-based wind power generation," *IEEE Trans. Autom. Sci. Eng.*, Vol. 99, No. 3, pp. 1–10 (2013).
20. Chwa, D. and K. B. Lee, "Variable structure control of the active and reactive powers for a DFIG in wind turbines," *IEEE Trans. Ind. Appl.*, Vol. 46, No. 6, pp. 2545–2555 (2010).
21. Camacho, E. F., and Bordons, C., *Model Predictive Control*, Springer, United Kingdom 2nd edn., (2004).
22. Thomas, J. L., S. Poullain, and A. Benchaib, "Analysis of a robust DC-bus voltage control system for a VSC-transmission scheme," *In Proc. 7th Int. Conf*, London, pp. 119–124 (2001).
23. Martinez, M. I., G. Tapia, A. Susperregui, and H. Camblong, "Sliding-mode control for DFIG rotor-and grid-side converters under unbalanced and harmonically distorted grid voltage," *IEEE Trans. Energy Convers.*, Vol. 27, No. 2, pp. 328–339 (2012).

Nasrin Kalamian graduated with a BSc and MSc from the Science and Technology University in Tehran. She is a control PhD student at Khaje Nasir University in Tehran. She worked on predictive methods on several applications including DFIGs and biped robots. Her current research interests are in predictive methods, nonlinear control, adaptive systems, identification, fault detection, and stochastic systems.

Mohammad Verij Kazemi was born in Nowshahr, Iran, in 1983. He received his BSc degree in electrical engineering from Gilan University, Gilan, Iran in 2006 and he received his MSc degree in electrical engineering from Sahand University of Technology, Tabriz, Iran in 2008. He is a PhD student at Noshivani University of Technology in Mazandaran, Iran. His research interests include electric machinery, motor control, power electronics, and renewable energy conversion.

Sayyed Asghar Gholamian was born in Babolsar, Iran, in 1976. He received his BSc degree in electrical engineering from K.N. Toosi University of Technology, Tehran, Iran in 1999 and his MSc degree in electric power engineering from the University of Mazandaran, Babol, Iran in 2001. He also received his PhD in electrical engineering from K.N. Toosi University of Technology, Tehran, Iran in 2008. He is currently Assistant Professor in the Department of Electrical Engineering at the Babol University of Technology, Iran. His research interests include power electronic and design, simulation, modeling, and control of electrical machines.